WILEY-VCH

DOI: 10.1002/macp.202000052 ((please add manuscript number))
Article type: Full Paper

A methodology of hydrodynamic complexity in topologically hyper-branched polymers undergoing hierarchical multiple relaxations

Haibao Lu[1,], Xiaodong Wang[1], Mokarram Hossain[2] and Yong Qing Fu[3]*

Prof. H. B. Lu and X. D. Wang
Science and Technology on Advanced Composites in Special Environments Laboratory, Harbin Institute of Technology, Harbin 150080, China
E-mail: luhb@hit.edu.cn
Dr. M. Hossain
Zienkiewicz Centre for Computational Engineering, College of Engineering, Swansea University, Swansea, UK
Prof. Y. Q. Fu
Faculty of Engineering and Environment, University of Northumbria, Newcastle upon Tyne, NE1 8ST, UK

Keywords: hyperbranched, thermodynamics, relaxation

A hydrodynamic model was proposed to describe conformational relaxation of molecules, viscoelasticity of arms and hierarchical multiple-shape memory effect (multi-SME) of hyper-branched polymer. Fox-Flory and Boltzmann's principles were employed to characterize and predict the hierarchical relaxations and their multi-SMEs in hyper-branched polymers. A constitutive relationship among relaxation time, molecular weight, glass transition temperature and viscoelastic modulus was then formulated. Results revealed that molecular weight and number of arms of the topologically hyper-branched polymers significantly influence their hydrodynamic relaxations and shape memory behaviors. The effectiveness of model has been demonstrated by applying it to predict mechanical and shape recovery behaviors of hyper-branched polymers, and the theoretical results show good agreements with the experimental ones. We expect this study provides an effective guidance on designing multi-SME in topologically hyper-branched polymers.

1. Introduction

Shape memory polymers (SMPs) are featured with shape memory effect (SME) which enables them being smart and responsive materials through shape deformation/recovery in the presence of external stimuli, such as thermal heating,[1] solvent,[2] light[3] or electrical fields.[4,5] SME is induced by partially segmental relaxation of macromolecular chains, where the hard segments are kept frozen to memorize the permanent conformation and the soft ones are kept active to undergo entropic conformation relaxation.[1] Multi-SMEs can be realized in the SMPs, in which the multi-step relaxation is introduced for the soft segments in the SMP macromolecules.[6] In practice, the first strategy for generating multi-SME is to generate the multiple segments by incorporating several discrete thermal transition components into polymer macromolecules.[6-8] The second one is to generate soft segments with a broad thermal transition in the polymer macromolecules.[9,10] Multi-SME in the SMPs has attracted extensive attention due to their capabilities of shape recovery step by step,[11] which creates great potentials for the practical applications in smart textiles, artificial intelligence robots, bio-medical engineering.[12,13]

Hyper-branched polymer is a popular functional material and consisted of multiple arms connected to a central core.[14,15] The core can be an atom, a molecule, or a macromolecule, while the arms are consisted of homogeneous or heterogeneous macromolecular chains. Generally, the homogeneous arms have equal lengths and uniform structures, whereas the heterogeneous ones have varied lengths and structures.[15] Recently, multi-SME has been discovered and explored in the homogeneous hyper-branched polymers. Due to their discrete thermal transitions of core and arms,[16] their shape recovery strength has been significantly enhanced.[17,18] As it is well known, modelling of the multi-SME in hyper-branched polymers is critical to explore their working mechanism and hydrodynamics.[1] However, this is difficult because their branch-to-branch topology structures and hydrodynamics are quite

different from those of their linear counterparts.[15] Till now, few theoretical studies have been carried out to study their hydrodynamic behaviors.

In this study, Fox-Flory equation[19] is initially employed to characterize the glass transition temperature (T_g) and relaxation behaviors of topologically hyper-branched polymers.[14] According to the Boltzmann's hydrodynamic principle,[20-22] a constitutive relationship is formulated with the consideration of molecular weight, number of arms, T_g and relaxation time. The proposed model is then employed to characterize and predict hierarchical and multiple relaxations (e.g., relaxations of the core and arms, respectively) and their multi-SMEs in hyper-branched polymers. Furthermore, effects of molecular weight and number of arms on hydrodynamic relaxations and shape memory behaviors of topologically hyper-branched polymers have been explored. Finally, the working principle of the complex multi-arms undergoing molecular-level hierarchical multiple relaxations is explored and discussed in order to link with the multi-SME in topologically hyper-branched polymers. Theoretically obtained results are compared with the experimental data reported in literature in order to verify the accuracy of proposed model. This study is expected to provide an effective strategy to explore the hydrodynamic principle of multi-SME in the topologically hyper-branched polymers.

2. Theoretical framework

The SME in amorphous SMPs occurs within the glass transition zone.[23] Here, T_g is an essential parameter for the hydrodynamics in the hyper-branched polymers.[24] The T_g of the hyper-branched polymer is determined by the number of arms (f) and molecular weight (M_n) based on the following equation:[19]

$$\begin{cases} T_g = T_g(\infty) - \dfrac{f}{2}\dfrac{B}{M_n} \\ M_n = M_0 + fM_a \end{cases} \tag{1}$$

where $T_g(\infty)$ is the T_g at M_n =+∞, B is a polymer-specific constant (the constant is proportional to the number of ends in the molecule), M_a and M_0 are the molecular weights of the arms and core of the hyper-branched polymer, respectively.

Figure 1 plots the calculated results of T_g based on equation (1) as functions of molecular weight (M_n) and number of arms (f). As revealed from **Figure 1(a)**, the molecular weight (M_n) has a significant influence on the T_g, which is increased from 320 *K* to 360 *K* with an increase M_n values from 0.5B to 1.0B at a given $T_g(\infty)$=400 *K*. As reported in literature,[25-27] the molecular weight has a significant influence on the T_g of the macromolecule chains, due to their constitutive relationships. Therefore, the T_g is gradually increased with an increase in molecular weight (M_n).

Meanwhile, effect of number of arms (f) on T_g has been investigated and the results are shown in **Figure 1(b)**. The analytical results reveal that the T_g is gradually decreased from 390 *K* to 370 *K* with an increase in the number of arms from f =2 to f =6, at a given molecular weight of $M_n = M_a$. While the T_g is gradually increased with an increase in the molecular weight ratio (M_0/M_a), mainly due to the increase in the molecular weight of core (M_0). It is found that there is a distinct difference in the effect of molecular weight on the T_g between the hyper-branched polymers and the conventional polymers with a sharp transition. The T_g of topologically hyper-branched polymer is not proportional to molecular weight, but determined by the number of arms. That is to say, the T_g will be increased with an increase in the molecular weight ratio of core and arms. However, it is then decreased with an increase in the number of arms at a given constant weight ratio.

[Figure 1]

To further investigate the influence of T_g on the relaxation of the SMPs as functions of temperature (T) and relaxation time (τ), the extended Arrhenius equation[28] is employed to characterize the topologically hyper-branched polymers, which is listed as following,

$$\ln \alpha_T(T) = \ln \frac{\tau}{\tau_0} = -\frac{AF_c}{k_b}\left(\frac{1}{T} - \frac{1}{T_g}\right) \quad (T < T_s) \tag{2}$$

where $\alpha_T(T)$ is the time-temperature superposition shift factor, τ_0 is the reference relaxation time, k_b is Boltzmann's constant, T_s is the transition temperature of arm segment, A is a material constant and F_c is the configurational free energy, which is a constant below the T_g as reported in Ref. [28].

Substituting equation (1) into (2), a constitutive relationship among the relaxation time, number of arms (f) and molecular weight of hyper-branched polymers (M_n) can be obtained,

$$\ln \frac{\tau}{\tau_0} = -\frac{AF_c}{k_b}\left(\frac{1}{T} - \frac{1}{T_g(\infty) - \frac{f}{2}\frac{B}{M_n}}\right) \quad (T < T_s) \tag{3}$$

A similar type of Equation (3) has previously been used to characterize the hydrodynamic behavior of arms in the hyper-branched polymers,[28] where T_s is the glass transition temperature of homogeneous arms. Pearson and Helfand[14] previously derived a specialized form for the viscosity (η) of hyper-branched polymers, where both the core and arms can be active when $T > T_s$,[29] e.g.:

$$\eta = \alpha M_a^{0.5} \exp(vM_a / M_0) \quad (T \geq T_s) \tag{4}$$

where α and v are given material constants, and are all proportional to the molecular weight of the arm.

It was reported that the volume (V_0) of core is significantly increased with an increase in temperature,[30] thus there is a constitutive relation between molecular weight and temperature which can be written as,

$$V_0 = \frac{k_b T}{G_0} \Rightarrow M_0 = \frac{\rho k_b T}{G_0} \tag{5}$$

where G_0 and ρ are the rubbery modulus and density of core, respectively.

By substituting equation (5) into (4), we can obtain the viscosity of the core (η) in hyper-branched polymers with respect to temperature as follows:

$$\eta = \alpha M_a^{0.5} \exp\left(\frac{\nu M_a G_0}{\rho k_b T}\right) \quad (T \geq T_s) \tag{6}$$

According to the equation (6), the relaxation time (τ) can be expressed by means of $\eta \approx E\tau$ (where E is the modulus and kept as a constant):[24]

$$\tau = \tau_0 \alpha M_a^{0.5} \exp\left(\frac{\nu M_a G_0}{\rho k_b T}\right) \quad (T \geq T_s) \tag{7}$$

Combining equations (3) and (7), the final form of relaxation time (τ) with respect to temperature within glass transition temperature zone can be obtained:

$$\tau = \begin{cases} \tau_0 \exp\left(-\dfrac{AF_c}{k_b}\left(\dfrac{1}{T} - \dfrac{1}{T_g(\infty) - \dfrac{f}{2}\dfrac{B}{M_n}}\right)\right) & (T < T_s) \\ \tau_0 \alpha M_a^{0.5} \exp\left(\dfrac{\nu M_a G_0}{\rho k_b T}\right) & (T \geq T_s) \end{cases} \tag{8}$$

Based on the equation (8), effects of the molecular weights of polymer and arms on the relaxation time with respect to temperature can be obtained and are presented in **Figure 2(a)** and **Figure 2(b)**, respectively. As revealed in **Figure 2(a)**, T_s is dramatically increased from 310.0 *K* to 345.3 *K* as the molecular weight of polymer (M_n) is increased from 0.5B to 0.9B,

at a given number of arms *f* =40. In the relaxation process of hyper-branched polymer, the relaxation of arms is initially induced with an increase in the temperature. With a further increase in temperature above T_s, the relaxation behavior of the core is activated, thus the higher molecular weight of the polymer is, the higher T_s can be achieved.

Meanwhile, the relaxation behavior of hyper-branched polymer as a function of temperature was investigated and the results are shown in **Figure 2(b)**. The analytical results revealed that the T_s is increased from 345.0 *K* to 370.1 *K* as the molecular weight of arm (M_a) is increased from 0.1B to 0.3B, at a given number of arms *f* =3. The T_s is significantly increased with an increase in the molecular weight of arm (M_a), which can be resulted from the increase in the viscosity and relaxation time. That is to say, the relaxation behavior of arm is critically determined by the molecular weight, of which a higher molecular weight is able to postpone the relaxation of arm, thus results in a longer relaxation time.

[Figure 2]

3. Multi-SME and hydrodynamics in hyper-branched polymer

3.1 SME in hyper-branched polymer

As mentioned above, the core and arms simultaneously undergo different relaxation behaviors when heated above T_s, thus resulting in a complex hydrodynamics in topologically hyper-branched polymer. Therefore, it is necessary to investigate the cooperative hydrodynamics of core and arms. Based on the concept of cooperative rearranging regions,[31,32] Adam and Gibbs have derived an expression of the relaxation time across glass transition region as follows:

$$\tau = \tau_0 \exp\left(\frac{\Delta H(T)}{RT}\right) = \tau_0 \exp\left(\frac{z(T)\Delta\mu}{RT}\right) \quad (9)$$

where ΔH is the enthalpy per molecule, R is gas constant, z is the domain size of the cooperative rearranging regions, and $\Delta\mu$ is the activation energy per molecule.

By substituting equation (9) into (8), the enthalpy per molecule can be written as:

$$\Delta H = \begin{cases} \left[-\dfrac{AF_c}{k_b}\left(\dfrac{1}{T} - \dfrac{1}{T_g(\infty) - \dfrac{f}{2}\dfrac{B}{M_n}} \right) \right] RT & (T < T_s) \\ \ln\left[\alpha M_a^{\,0.5} \exp\left(\dfrac{\nu M_a G_0}{\rho k_b T} \right) \right] RT & (T \geq T_s) \end{cases} \tag{10}$$

Based on the phase transition theory,[22] the phase evolution function (ϕ_f) can be expressed using the enthalpy parameter as following:[33]

$$\phi_f(T) = \frac{\varepsilon_s}{\varepsilon_{pre}} = 1 - \beta T \exp\left(-\frac{\Delta H}{RT} + \frac{T_h - T}{bT_h - T} \right) \tag{11}$$

where β and b are the given material constants, T_h is the temperature when stored strain (ε_s) is released completely, and ε_{pre} is the pre-strain in polymer.

According to equations (10) and (11), the final expression of phase evolution function (ϕ_f) can be written as:

$$\phi_f(T) = \begin{cases} 1 - \beta T \exp\left[-\dfrac{AF_c}{k_b}\left(\dfrac{1}{T} - \dfrac{1}{T_g(\infty) - \dfrac{f}{2}\dfrac{B}{M_n}} \right) + \dfrac{T_h - T}{bT_h - T} \right] & (T < T_s) \\ 1 - \beta T \exp\left\{ -\ln\left[\alpha M_a^{\,0.5} \exp\left(\dfrac{\nu M_a G_0}{\rho k_b T} \right) \right] + \dfrac{T_h - T}{bT_h - T} \right\} & (T \geq T_s) \end{cases} \tag{12}$$

To verify the proposed model, the analytical results obtained using equation (12) were compared with the experimental data of epoxy-based hyper-branched SMP reported in Ref. [22], and the results are shown in **Figure 3**. All the parameters used in the equation (12) are listed in **Table 1**. Results show that the hyper-branched SMP undergoes Arrhenius-typed and

non-Arrhenius-typed relaxation behaviors below T_s (e.g., from 305 *K* to 339 *K*) and above T_s (e.g., from 339 *K* to 355 *K*), respectively, where T_s =339 *K*. The analytical results are in good agreement with the experimental data of the hyper-branched SMP.

[Table 1]/[Figure 2]

Based on the study reported in Ref. [22], the SME in SMP is originated from phase transition from a frozen state to an active one of the soft segments, where the hard segments are kept frozen. During the phase transition of hyper-branched polymer, the cores in the polymer are assumed to work as hard segments which do not show any phase transitions. While the arms work as soft segments and undergo phase transitions. Here, the SME in the hyper-branched polymer is originated from the phase transition of arms. Therefore, the proposed model is applicable to characterize and predict the hydrodynamic relaxation of the hyper-branched SMP.

To further investigate the relaxation behavior of topologically hyper-branched SMP, effects of molecular weight (M_n), number of arms (f) and T_g were investigated and the results are plotted in **Figure 4**. **Figure 4(a)** shows the effect of molecular weight on the stored strain. The T_g is gradually increased from 332 *K*, 343 *K*, 350 *K*, 355 *K* to 360 *K* with an increase in the molecular weight (M_n) from 0.5B, 0.6B, 0.7B, 0.8B to 0.9B, where the number of arms is kept a constant. Meanwhile, the effect of number of arms on stored strains has been plotted in **Figure 4(b)**. It is revealed that the T_g is gradually decreased from 390 *K*, 380 *K*, 370 *K*, 360 *K* to 350 *K* with an increase in the number of arms (f) from 10, 20, 30, 40 to 50, where the molecular weight is kept a constant. These analytical results identify that the T_g and relaxation behavior are critically determined by the molecular weight and number of arms. With a higher molecular weight and fewer number of arms, the polymer has a higher T_g, due to the significant increase in viscosity of hyper-branched SMP.

[Figure 4]

3.2. Hydrodynamic behavior of hyper-branched polymer

As the hyper-branched polymer is incorporated with both the core and arms, Gordon-Taylor rule[22,34] is therefore employed to characterize the storage modulus ($E(T)$):

$$\frac{1}{E(T)} = \frac{\phi_f(T)}{E_f(T)} + \frac{1-\phi_f(T)}{E_a} \tag{13}$$

where $E_f(T)$ and E_a are the moduli of the frozen core and active arms of the hyper-branched polymer, respectively.

The storage modulus of the frozen core ($E_f(T)$) has the following relationship with temperature:[35]

$$\log E_f(T) = \log E(T^{ref}) - \gamma(T - T^{ref}) \tag{14}$$

where $E(T^{ref})$ is the modulus at the reference temperature T^{ref} , and parameter γ is a material constant.

According to the analytical results obtained from equation (14), effects of molecular weight (M_n) and number of arms (f) on the storage modulus are shown in **Figure 5**, in which the constitutive relationships among storage moduli, molecular weight and number of arms for the topologically hyper-branched SMP with various T_g have been presented. As shown in **Figure 5(a)**, the storage modulus ($E(T)$) is increased from 735 MPa, 841 MPa, 882 MPa, 902 MPa to 918 MPa with an increase in molecular weight (M_n) from 0.5*B*, 0.6*B*, 0.7*B*, 0.8*B* to 0.9*B*, at a given number of arms (f =40). On the other hand, the storage modulus ($E(T)$) is gradually decreased from 950 MPa, 937 MPa, 916 MPa, 880 MPa to 817 MPa with an increase in number of arms (f) from 10, 20, 30, 40 to 50, at a given molecular weight (M_n =0.5*B*), as shown in **Figure 5(b)**.

[Figure 5]

To verify the proposed model, the analytical results of storage modulus of the SMP obtained using equations (13) and (14) are plotted as a function of temperature, and then the results are compared with the experimental data reported in Ref. [22] as shown in **Figure 6**. The parameters used in the equations (13) and (14) are listed in **Table 2**. It is revealed that the storage modulus is rapidly decreased from 834 MPa to 86 MPa with an increase in temperature from 305 *K* to 339 *K*. Then the storage modulus is then decreased slowly from 86 MPa to 10 MPa with a further increase in temperature from 339 *K* to 355 *K*. These analytical results clearly show that the hyper-branched SMP undergoes two types of thermomechanical relaxations, i.e., Arrhenius-typed and non-Arrhenius-typed relaxations. The thermomechanical relaxation of the arms in the hyper-branched SMP is governed by the Arrhenius equation and determined by active energy and temperature, whereas that of the core is determined by the molecular weight and number of arms.

[Table 2]/[Figure 6]

The hyper-branched SMP presents a unique SME in comparison with the conventional ones, whose SME is resulted from phase transition of the segments and ruled by the Arrhenius and Williams-Landel-Ferry (WLF) equations.[29] Whereas the SME in the hyper-branched SMPs is originated from the molecular-level hierarchical regression of arms and core and determined by the temperature, relaxation time, molecular weight and number of arms. In the hyper-branched SMPs, the SME is initially induced by the hydrodynamic relaxation of the arms and ruled by the Arrhenius equation. Then the relaxation of core is consequently activated and determined by a cooperative interaction within the arms, and the relaxation is not only determined by molecular weight of core, but also determined by number of arms.

3.3. Multi-SME and hydrodynamics in hyper-branched polymer

Furthermore, the working principle of multi-SME and hydrodynamics for the hyper-branched polymer have been studied. Based on the Boltzmann's hydrodynamics, stored strain

relaxation of the hyper-branched polymer with multiple segments can be obtained using the following equation:[36,37]

$$\varepsilon_s = \sum_{i=1}^{n} \phi_{fi}(T)\varepsilon_{prei} \tag{15}$$

where n is the number of arms, subscript i and ε_{prei} represent the relaxation and pre-loading strain of the *i*th type of multi-arm, respectively.

Substituting equation (12) into equation (15), we can obtain an equation to characterize the quadruple-SME in the hyper-branched SMP incorporated of a core and three types of multi-arms. **Figure 7(a)** illustrates the molecular structure of topologically hyper-branched SMP with a variety of number of multi-arms $f_1 = f_2 = f_3 = 20$. As shown in **Figure 7(b)**, the glass transition temperature (T_{g2}) is gradually increased from 333 *K* to 380 *K* with an increase in the molecular weight (M_{n2}) from 0.15*B* to 0.5*B*, where the numbers of three types of multi-arms are $f_1 = f_2 = f_3 = 20$, $M_{n1} = B$ and $M_{n3} = 0.1B$. These has resulted in the constant values of T_{g1}=390 *K* and T_{g3}=300 *K* (as presented by the first and last triangle marks). On the other hand, **Figure 7(c)** illustrates the molecular structure of topologically hyper-branched SMP with a variety of molecular weights of $M_{n1} = M_{n2} = M_{n3} = 0.5B$. The glass transition temperature (T_{g2}) is decreased from 380 *K* to 340 *K* with an increase in the number of arm (f_2) from 20 to 60, as shown in **Figure 7(d)**. While the T_{g1}=390 *K* and T_{g3}=330 *K* are kept as constants, which are resulted from values of f_1=10 and f_3=70. These analytical results reveal that the quadruple stored strain relaxations and their quadruple-SMEs in hyper-branched SMP can be well characterized and predicted, using our proposed model.

To further explore the hydrodynamics in hyper-branched SMPs, the Takayanagi principle[38] is employed to investigate the hydrodynamic behavior, and the storage modulus ($E(T)$) can be expressed as:

$$E(T) = 1/\sum_{i=1}^{n} \frac{\lambda_i}{E_i(T)} = 1/\sum_{i=1}^{n} \left[\lambda_i \left(\frac{\phi_{fi}(T)}{E_{fi}(T)} + \frac{1-\phi_{fi}(T)}{E_{ai}} \right) \right] \quad \left(\sum_{i=1}^{n} \lambda_i = 1 \right) \tag{16}$$

where λ_i is the weight fraction of the *i*th type of multi-arm, $E_{fi}(T)$ and E_{ai} are the moduli at frozen and active states, respectively.

[Figure 7]

As shown in **Figure 8(a)** and **Figure 8(b)**, the storage modulus is gradually increased from 553 MPa to 790 MPa with an increase in the weight fraction (λ_3) from 33% to 80%, where T_{g3}=390 *K*. Meanwhile, the storage moduli are decreased to 30 MPa and 90 MPa, respectively, for the first-step transition state of hyper-branched SMP. The minimal storage modulus is decreased to a constant value of 10 MPa, although the weight fraction of multi-arm is varied. The simulation results clearly reveal that the weight fractions of different types of multi-arm components have critical roles to determine storage modulus and hydrodynamic behaviors of hyper-branched SMP.

On the other hand, the storage modulus is generally used to characterize the SMP, and investigate their shape recovery behaviors. As revealed from **Figure 8**, the hyper-branched SMP undergoes three thermal transitions at different temperatures of T_{g1}, T_{g2} and T_{g3}, respectively, whereas the storage modulus is significantly decreased. These analytical results show that the transition temperature is critically determined by the molecular weight, and T_{g2} is increased from 333 *K* to 380 *K* when the molecular weight of M_{n2} is increased from 0.15*B* to 0.5*B*. Therefore, these curves are helpful to describe and predict the shape recovery behavior of hyper-branched SMPs. All the above results confirm that our proposed model

provides a promising approach for design and control of the multi-SME in topologically hyper-branched polymers.

[Figure 8]

4. Conclusions

In this study, we propose a theoretical framework to investigate the working mechanism in SME and hydrodynamic principle of hyper-branched polymers. It is demonstrated that the proposed constitutive model is able to describe and predict their shape memory behaviors and hierarchical multiple relaxations. It provides an effective way to characterize the dependences of hydrodynamic behaviors on the molecular weight, number of arms, glass transition temperature functions. The conformational relaxation of molecules and viscoelasticity of hyper-branched arms have been identified as the driving force for the SME and multi-SME in hyper-branched polymers. The accuracy of analytical results is examined by experimental ones, which have been well fitted. This newly proposed model is expected to provide an effective strategy to explore the hydrodynamic principle in multi-SME of topologically hyper-branched polymers.

Acknowledgements

This work was financially supported by the National Natural Science Foundation of China (NSFC) under Grant No. 11672342 and 11725208, Newton Mobility Grant (IE161019) through Royal Society and NFSC.

Received: ((will be filled in by the editorial staff))
Revised: ((will be filled in by the editorial staff))
Published online: ((will be filled in by the editorial staff))

References

[1] J. Hu, Y. Zhu, H. Huang and J. Lu *Prog. Polym. Sci.* **2012**, *37*, 1720.

[2] G. I. Peterson, E. P. Childers, H. Li, A. V. Dobrynin and M. L. Becker *Macromolecules* **2017**, *50*, 4300.

[3] S. Ji, F. Fan, C. Sun, Y. Yu and H. Xu *ACS Appl. Mater. Interfaces* **2017**, *9*, 33169.

[4] R. Mohr, K. Kratz, T. Weigel, M. Lucka-Gabor, M. Moneke and A. Lendlein *Proc. Natl. Acad. Sci.* **2006**, *103*, 3540.

[5] M. Y. Razzaq, M. Anhalt, L. Frormann and B. Weidenfeller *Mat. Sci. Eng. A-Struct* **2007**, *444*, 227.

[6] M. Y. Razzaq, M. Behl, K. Kratz and A. Lendlein *Adv. Mater.* **2013**, *25*, 5514.

[7] T. Xie, X. Xiao and Y. T. Cheng *Macromol. Rapid. Comm.* **2009**, *30*, 1823.

[8] A. H. Torbati, H. B. Nejad, M. Ponce, J. P. Sutton and P. T. Mather *Soft Matter* **2014**, *10* 3112.

[9] T. Xie *Nature* **2010**, *464*, 267.

[10] J. Li and T. Xie *Macromolecules* **2011**, *44*, 175.

[11] R. Hoeher, T. Raidt, C. Krumm, M. Meuris, F. Katzenberg and J. C. Tiller *Macromol. Chem. Phys.* **2013**, *214*, 2725.

[12] R. Xiao and C. S. Tian *J. Mech. Phys. Solids* **2019**, *125*, 472.

[13] H. B. Lu and S. Y. Du *Polym. Chem.* **2014**, *5*, 1155.

[14] D. S. Pearson and E. Helfand *Macromolecules* **1984**, *17*, 888.

[15] C. N. Likos, H. Löwen, M. Watzlawek, B. Abbas, O. Jucknischke, J. Allgaier and D. Richter *Phys. Rev. Lett.* **1998**, *80*, 4450.

[16] C. Mayer, F. Sciortino, C. N. Likos, P. Tartaglia, H. Löwen and E. Zaccarelli *Macromolecules* **2009**, *42*, 423.

[17] T. Liu, J. Li, Y. Pan, Z. Zheng, X. Ding and Y. Peng *Soft Matter* **2011**, **7**, 1641.

[18] M. Bothe, K. Y. Mya, E. M. Jie Lin, C. C. Yeo, X. Lu, C. He and T. Pretsch *Soft Matter* **2012**, *8*, 965.

[19] A. Kisliuk, Y. Ding, J. Hwang, J. S. Lee, B. K. Annis, M. D. Foster and A. P. Sokolov *J. Polym. Sci. Pol. Phys.* **2002**, *40*, 2431.

[20] X. D. Wang, Y. H. Liu, H. B. Lu, N. Wu, D. Hui and Y. Q. Fu *Polymer* **2019**, *181*, 121785.

[21] X. D. Wang, H. B. Lu, N. Wu, D. Hui, M. J. Chen and Y. Q. Fu **2019**, *Smart Mater. Struct. 28*, 085011.

[22] Y. Liu, K. Gall, M. L. Dunn, A. R. Greenberg and J. Diani *Int. J. Plasticity* **2006**, *22*, 279.

[23] Q. Meng and J. Hu *Compos. Part A-Appl. Sci. Manuf.* **2009**, *40*, 1661.

[24] M. H. Cohen and G. S. Grest *Phys. Rev. B* **1979**, *20*, 1077.

[25] Y. Xiang, D. Zhong, P. Wang, G. Mao, H. Yu and S. Qu *J. Mech. Phys. Solids.* **2018**, *117*, 110.

[26] D. Zhong, Y. Xiang, T. Yin, H. Yu and S. Qu *Int. J. Solids. Struct.* **2019**, *176*, 121.

[27] Y. Xiang, D. Zhong, P. Wang, T. Yin, H. Zhou, H. Yu, C. Baliga, S. Qu and W. Yang *J. Mech. Phys. Solids.* **2019**, *128*, 208.

[28] P. A. O'Connell and G. B. McKenna *J. Chem. Phys.* **1999**, *110*, 11054.

[29] K. Yu, T. Xie, J. S. Leng, Y. Ding and H. J. Qi *Soft Matter* **2012**, *8*, 5687.

[30] R. C. Ball and T. C. B. McLeish *Macromolecules* **1989**, *22*, 1911.

[31] C. A. Solunov *Eur. Polym. J.* **1999**, *35*, 1543.

[32] G. Adam and J. H. Gibbs *J. Chem. Phys.* **1965**, *43*, 139.

[33] H. B. Lu, X. D. Wang, Y. T. Yao and Y. Q. Fu *Smart Mater. Struct.* **2018**, *27*, 065023.

[34] H. B. Lu, X. D. Wang, Z. Y. Xing and Y. Q. Fu *J. Phys. D Appl. Phys.* **2019**, *52*, 245301.

[35] E. M. Arruda and M. C. Boyce *Int. J. Plasticity* **1993**, *9*, 697.

[36] X. D. Wang, W. Jian, H. B. Lu, D. Lau and Y. Q. Fu *Macromolecules* **2019**, *52*, 6045.

[37] X. D. Wang, H. B. Lu, X. J. Shi, K. Yu and Y. Q. Fu *Compo. Part B: Eng.* **2019**, *160*, 298.

[38] C. Lai, R. Ayyer, A. Hiltner and E. Baer *Polymer* **2010**, *51*, 1820.

Figure Caption

Figure 1. (a) Analytical results for the T_g as a function of number of arms (f) at a given M_n =0.5*B*, 0.6*B*, 0.7*B*, 0.8*B*, 0.9*B* and 1.0*B* (g/mol). **(b)** Analytical results for the T_g with respect to molecular weight ratio (M_0/M_a) at a given *f*=2, 3, 4, 5 and 6.

Figure 2. Analytical results of relaxation time (τ/τ_0) as a function of temperature of hyper-branched polymer. **(a)** At a given M_n =0.5*B*, 0.6*B*, 0.7*B*, 0.8*B* and 0.9*B*. **(b)** At a given M_a =0.1*B*, 0.15*B*, 0.2*B*, 0.25*B* and 0.3*B*.

Figure 3. Comparison of theoretical results and experimental data[22] for the stored strain with respect to temperature of epoxy-based hyper-branched SMP.

Figure 4. Analytical results based on equation (12) for the dimensionless stored strain ($\varepsilon_s/\varepsilon_{pre}$) as a function of temperature of hyper-branched SMP. **(a)** At a given molecular weight of M_n =0.5*B*, 0.6*B*, 0.7*B*, 0.8*B* and 0.9*B*. **(b)** At a given number of arms of f =10, 20, 30, 40 and 50.

Figure 5. Analytical results of storage modulus as a function of temperature. **(a)** At M_n =0.5*B*, 0.6*B*, 0.7*B*, 0.8*B* and 0.9*B*. **(b)** At f =10, 20, 30, 40 and 50.

Figure 6. Comparison of storage modulus as a function of temperature between the analytical results of equation (14) and experimental data.[22]

Figure 7. **(a)** Illustrations of the molecular structure of topologically hyper-branched SMP with a variety of number of multi-arms $f_1 = f_2 = f_3$ =20. **(b)** Numerical analysis of the influence of temperature on the stored strain relaxation at a molecular weight of M_{n2} =0.15*B*, 0.2*B*, 0.3*B*, 0.4*B*, and 0.5*B*. **(c)** Illustrations of the molecular structure of topologically hyper-branched SMP with a variety of molecular weights of $M_{n1} = M_{n2} = M_{n3}$ =0.5*B*. **(d)** Numerical

analysis of the influence of temperature on the stored strain relaxation at a number of arm of f_2 =20, 30, 40, 50, and 60.

Figure 8. Analytical analysis of the influence of temperature on the storage modulus. **(a)** At a weight fraction of $\lambda_1 = \lambda_2 = \lambda_3$ =1/3. **(b)** At a weight fraction of λ_1 =0.1, λ_2 =0.2 and λ_3 =0.7.

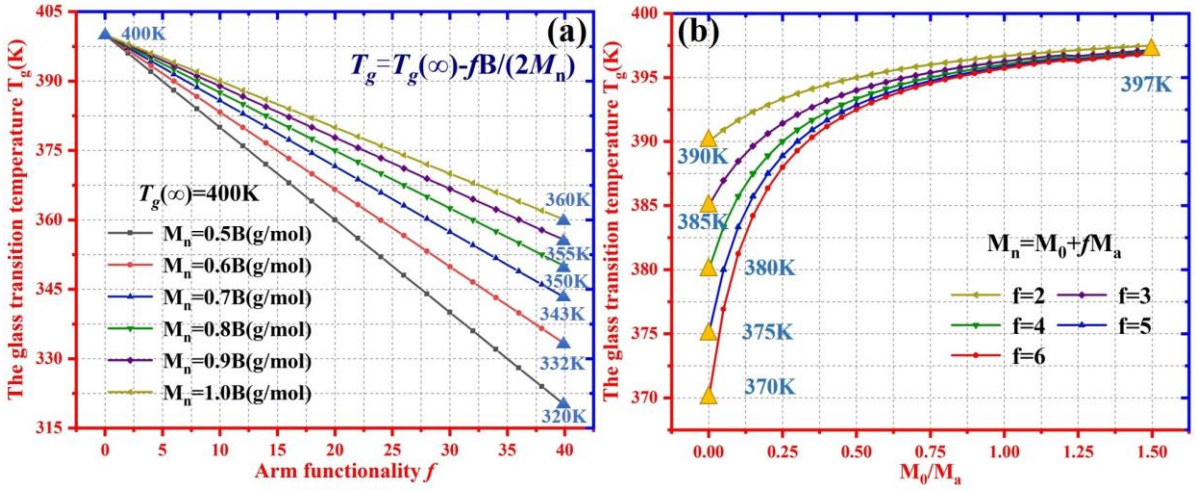
(a)
T_g=T_g(∞)-fB/(2M_n)
T_g(∞)=400K
M_n=0.5B(g/mol)
M_n=0.6B(g/mol)
M_n=0.7B(g/mol)
M_n=0.8B(g/mol)
M_n=0.9B(g/mol)
M_n=1.0B(g/mol)
400K
360K
355K
350K
343K
332K
320K
The glass transition temperature T_g(K)
Arm functionality f
(b)
M_n=M_0+$f$$M_a$
f=2
f=3
f=4
f=5
f=6
397K
390K
385K
380K
375K
370K
The glass transition temperature T_g(K)
M_0/M_a

Figure 1.

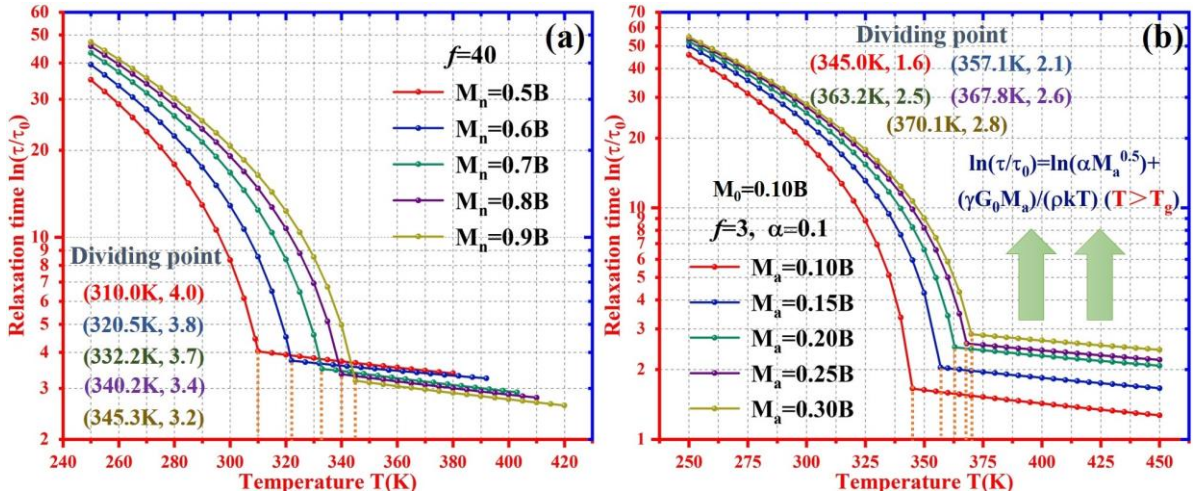
(a)
f=40
Mn=0.5B
Mn=0.6B
Mn=0.7B
Mn=0.8B
Mn=0.9B
Dividing point
(310.0K, 4.0)
(320.5K, 3.8)
(332.2K, 3.7)
(340.2K, 3.4)
(345.3K, 3.2)
Relaxation time ln(τ/τ0)
Temperature T(K)
(b)
Dividing point
(345.0K, 1.6)
(357.1K, 2.1)
(363.2K, 2.5)
(367.8K, 2.6)
(370.1K, 2.8)
ln(τ/τ0)=ln(αMa0.5)+
(γG0Ma)/(ρkT) (T>Tg)
M0=0.10B
f=3, α=0.1
Ma=0.10B
Ma=0.15B
Ma=0.20B
Ma=0.25B
Ma=0.30B
Relaxation time ln(τ/τ0)
Temperature T(K)

Figure 2.

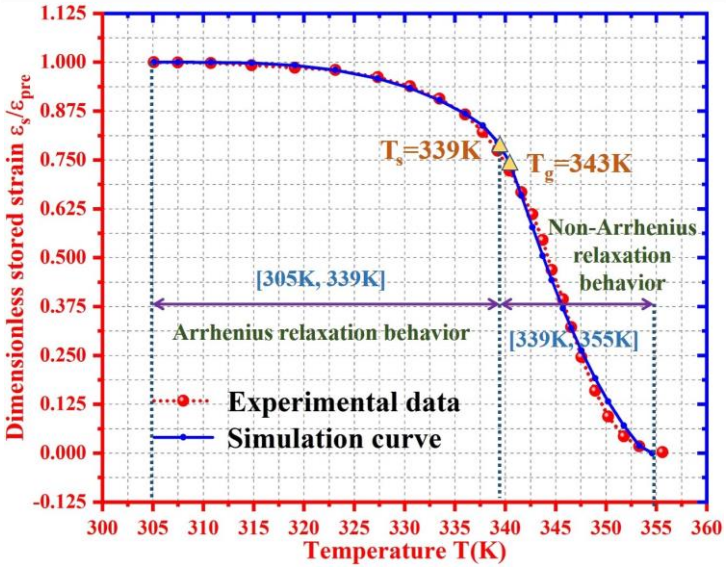
Dimensionless stored strain $\varepsilon_s/\varepsilon_{pre}$
Temperature T(K)
T_s=339K
T_g=343K
Non-Arrhenius relaxation behavior
[305K, 339K]
Arrhenius relaxation behavior
[339K, 355K]
Experimental data
Simulation curve

Figure 3.

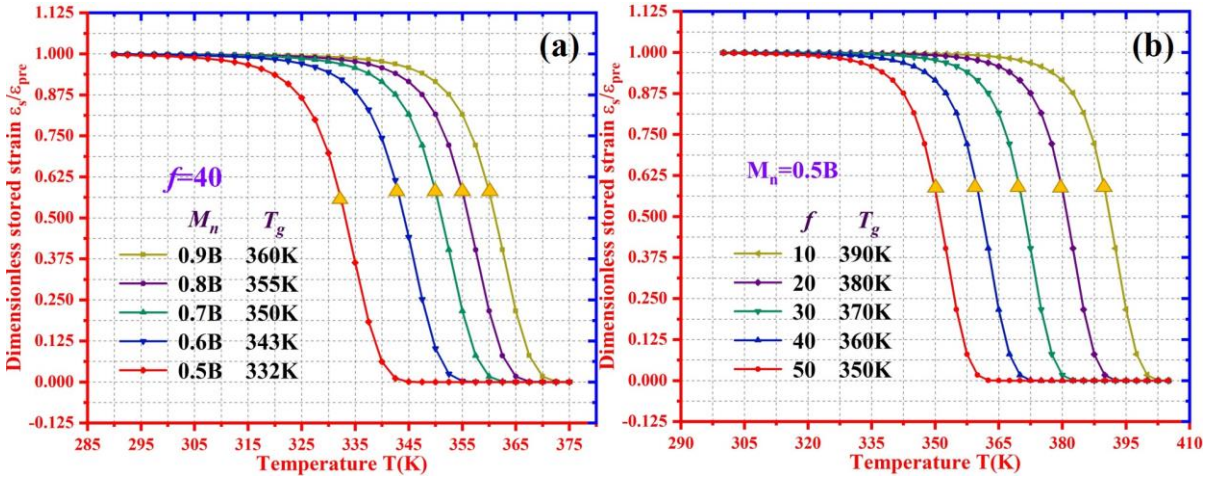
(a)
f=40
Mn Tg
0.9B 360K
0.8B 355K
0.7B 350K
0.6B 343K
0.5B 332K
Dimensionless stored strain εs/εpre
Temperature T(K)
(b)
Mn=0.5B
f Tg
10 390K
20 380K
30 370K
40 360K
50 350K
Dimensionless stored strain εs/εpre
Temperature T(K)

Figure 4.

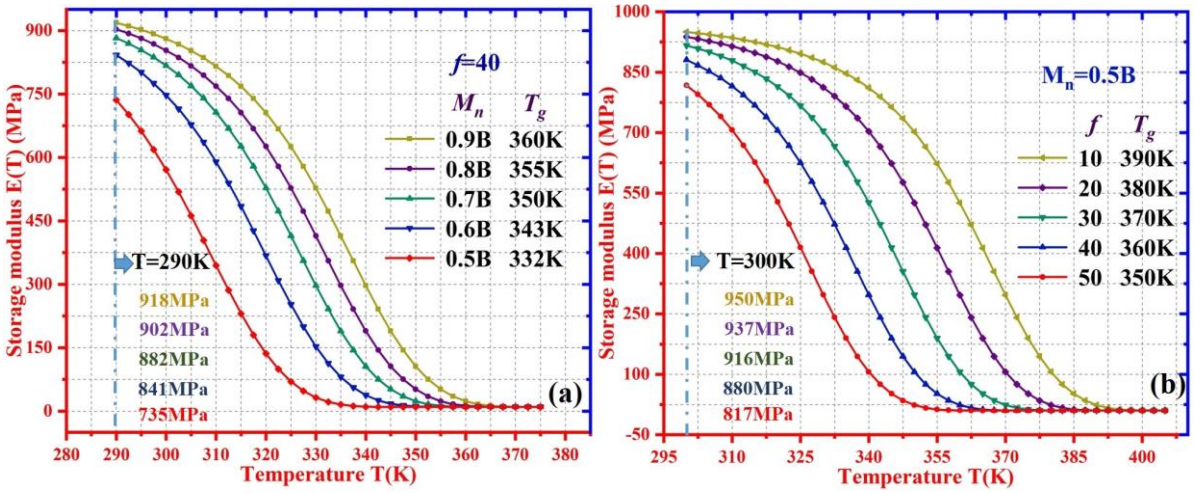
Storage modulus E(T) (MPa)
Temperature T(K)
f=40
Mn Tg
0.9B 360K
0.8B 355K
0.7B 350K
0.6B 343K
0.5B 332K
T=290K
918MPa
902MPa
882MPa
841MPa
735MPa
(a)
Mn=0.5B
f Tg
10 390K
20 380K
30 370K
40 360K
50 350K
T=300K
950MPa
937MPa
916MPa
880MPa
817MPa
(b)

Figure 5.

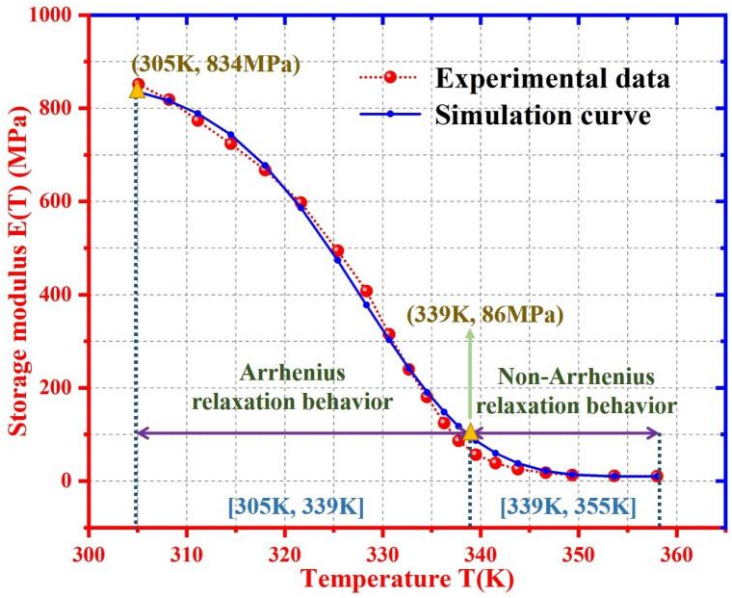
(305K, 834MPa)
Experimental data
Simulation curve
(339K, 86MPa)
Arrhenius
relaxation behavior
Non-Arrhenius
relaxation behavior
[305K, 339K]
[339K, 355K]
Storage modulus E(T) (MPa)
Temperature T(K)
1000
800
600
400
200
0
300
310
320
330
340
350
360

Figure 6.

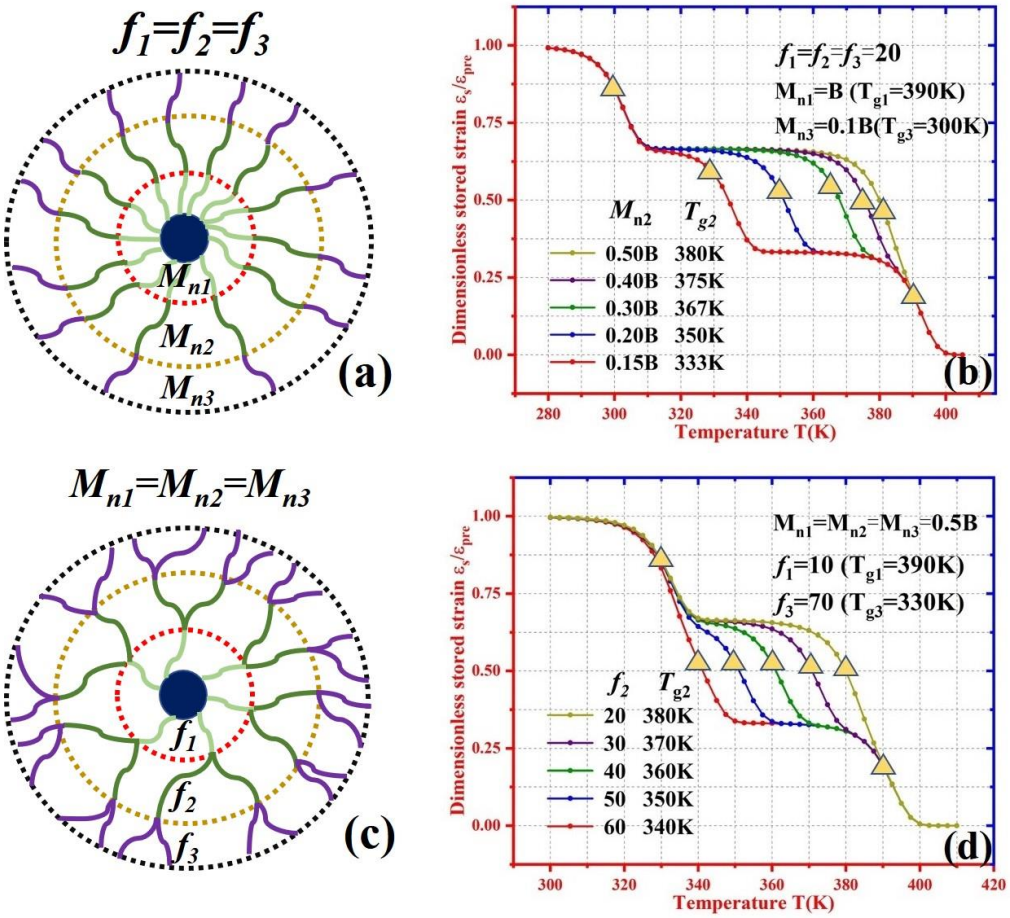
f1=f2=f3
Mn1
Mn2
Mn3
(a)
Dimensionless stored strain εs/εpre
1.00
0.75
0.50
0.25
0.00
f1=f2=f3=20
Mn1=B (Tg1=390K)
Mn3=0.1B(Tg3=300K)
Mn2 Tg2
0.50B 380K
0.40B 375K
0.30B 367K
0.20B 350K
0.15B 333K
(b)
280 300 320 340 360 380 400
Temperature T(K)
Mn1=Mn2=Mn3
f1
f2
f3
(c)
Mn1=Mn2=Mn3=0.5B
f1=10 (Tg1=390K)
f3=70 (Tg3=330K)
f2 Tg2
20 380K
30 370K
40 360K
50 350K
60 340K
(d)
300 320 340 360 380 400 420
Temperature T(K)

Figure 7.

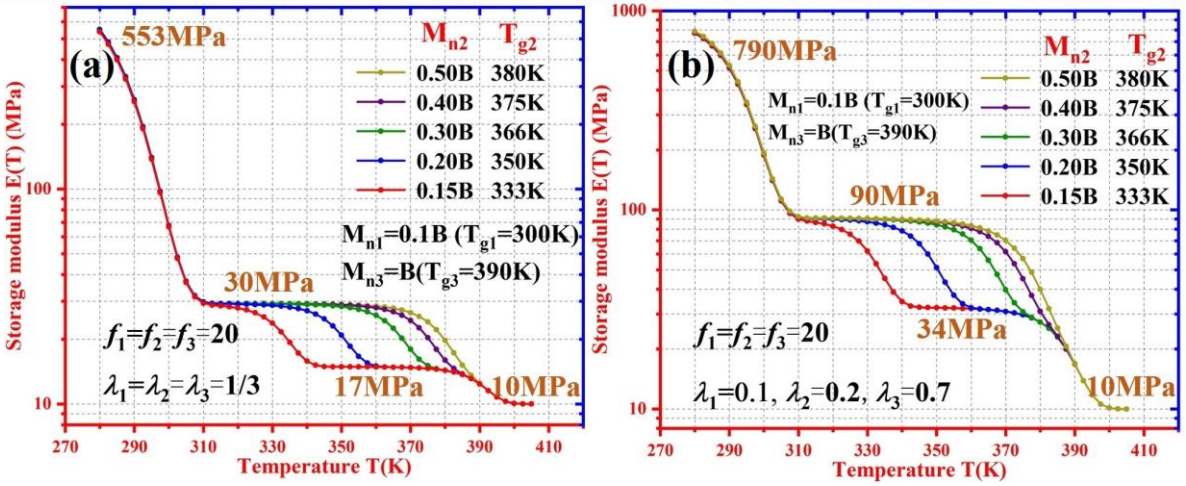
(a)
553MPa
30MPa
17MPa
10MPa
M_{n2} T_{g2}
0.50B 380K
0.40B 375K
0.30B 366K
0.20B 350K
0.15B 333K
M_{n1}=0.1B (T_{g1}=300K)
M_{n3}=B(T_{g3}=390K)
f_1=f_2=f_3=20
λ_1=λ_2=λ_3=1/3
Storage modulus E(T) (MPa)
Temperature T(K)
(b)
790MPa
90MPa
34MPa
10MPa
M_{n1}=0.1B (T_{g1}=300K)
M_{n3}=B(T_{g3}=390K)
f_1=f_2=f_3=20
λ_1=0.1, λ_2=0.2, λ_3=0.7
Storage modulus E(T) (MPa)
Temperature T(K)

Figure 8.

Table Caption

Table 1. Values of parameters used in equation (12).

Table 2. Values of parameters used in equations (13) and (14).

Table 1.

β	AF_c / k_b	$b(T<T_s)$	$T_s(K)$	$\alpha M_a^{0.5}$	$vM_aG_0 / \rho k_b$	$b(T \geq T_s)$
0.00115	7251.812	0.842	339.210	0.00029	3255.810	0.924

Table 2.

$E(T^{ref})(MPa)$	γ (MPa/K)	$T^{ref}(K)$	$E_a(MPa)$	$\phi_f(T)$
1002.03	0.0001	202.06	10	0.895